# Infante's Structural Model: Preliminary Design Process and Analysis

Nuno Maria Mota Paiva de Andrada
nuno.andrada@tecnico.ulisboa.pt

Instituto Superior Técnico, Universidade de Lisboa, Portugal

June 2019

**Abstract**

Over the last couple of decades there has been a paradigm shift in the space sector. Large and expensive satellites with long operation cycles are being replaced by constellations of smaller and cheaper ones with shorter lifetime cycles, faster developed and manufacture times, and easily replaced in case of failure. This paradigm shift is motivated by the standardization of the cubesat design and by developments in the mobile, automotive and computer industries which result in smaller, lighter, cheaper and more powerful electronic components as well as in new manufacturing techniques and technologies. These factors have made it financially viable for private companies to invest in the space industry and services. INFANTE is a pioneer Portuguese Research and Development (R&D) project that appears in the context of the "New Space" era. It is divided in two areas, Space and Ground. The Space segment includes a low cost smallsat platform for Earth observation (EO) applications. This work focuses on the satellite's structural subsystem development up to the preliminary design review (PDR). First, a cubesat structure state of the art is presented and is used as market study to derive different solution concepts. Then, several trade-offs concerning major design points are discussed. Afterwards, a computational model is derived to study the structure's behaviour by performing static, modal, harmonic response and random vibrations analyses. The applied loads were provided by the launch vehicle entity (LVE). After discussing the analysis results, the conclusions are presented and future work proposals are made.
**Keywords:** Smallsat, Structure, Design Development, Static Analysis, Dynamic analysis, Preliminary design review

## 1. Introduction

The main objective of this paper is to document the development of INFANTE's 16U structural subsystem up to preliminary design review. This work explores the cubesat structure state of the art which is used as benchmark to then address major design aspects, considerations and trade-offs made during the preliminary design process. Following, a computer-aided design (CAD) model is developed using SolidWorks 2016. To study the model's behaviour when subjected to the launcher loads, quasi-static and dynamic simulations are performed using ANSYS 18.1 software.

INFANTE is a Portuguese R&D project that appears in the context of the New Space era where small satellites and massive constellations lead the way of space access. The project proposes the design, production, launch and operation of a small satellite based on the cubesat standards which is intended to be a precursor of a constellation for maritime surveillance, Earth observation and communications between satellites and ground stations.

This is a pioneer project in Portugal given it's magnitude and the number of parties involved. In total 20 entities, from companies, to R&D centres, institutes and international organizations, form a consortium, lead by Tekever, which will launch the first satellite completely designed, manufactured and operated solely by the Portuguese industry.

The space industry has been evolving, moving towards a democratization. According to nanosats.eu, a nanosat database that keeps records of missions, constellations, new technologies, launch providers and many more detailed information, the number of launched nanosatellites has been steadily increasing from just two in 1998 to more than two hundred in 2017 and in 2018. Figure 1, shows the number of launched nanosatellites in the period between 1998 and 2018 and the predictions made by Nanosats Database and SpaceWorks, compiled by Nanosats Database. Nanosats Database [1] predicts that in the next six years more than three thousand nanosatellites will be launched, more than five hundred of which will be launched in 2019 alone. It is possible to see that the tendency is for the nanosatellite launch numbers to keep increasing and

it is predicted that in 2023 will be launched more than 700 nanosatellites.

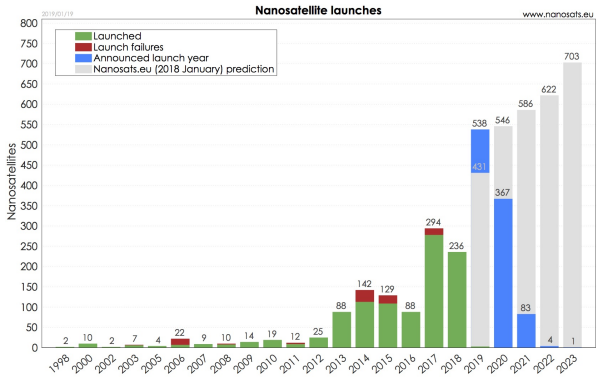


Figure 1: Nanosatellites launches between 1998 and 2023 - Including nanosats.eu predictions (Adapted from [1])

The increasing number of operating nanosatellites, have remarkable repercussions in both the commercial and the scientific world. By having access to Space, universities are able to test a wide variety of payloads in orbit that otherwise would not be possible for most of them, therefore, pushing the scientific boundaries further at each launch. With the increasing number of companies flying their nanosatellites for commercial applications, like Planet, Spire, OneWeb and many others, the consumer will benefit from the market competition where better and cheaper products are already improving areas like agriculture, fishery, weather forecast, broadband internet or Internet of Things (IoT).

### 1.1. Cubesat Structures State of the Art

Cubesats are small satellites specially used by universities, schools and private companies for research, experiment and business purposes. A cubesat is composed by one or more 10cm x 10cm x 11.35cm units (U) and each unit weights up to 1.33Kg [4]. The most common cubesats are 1U, 2U and 3U, but there are larger configurations. It is fairly common for these kind of satellites to use off-the-shelf (COTS) electronic and structural components. This allows for a rapid and cheap development of subsystems. These satellites expanded the ride-share market. It is not financially viable to purchase a primary flight slot. The solution adopted is to buy a secondary flight slot on an already scheduled flight. However, the cubesat owner is subjected to the conditions agreed by the LVE and the primary satellite owner such as the launch time window, the deployment orbit or the safety requirements imposed by both entities. To minimize the risk of damaging the primary satellite, cubesats may be launched inside pods, such as the Poly Picosatellite Orbital Deployer (P-POD) [3] standardized deployment system developed by Cal Poly.

Traditionally, satellite structures are designed considering the requirements of a specific mission, therefore, a given structure cannot fit in satellites for different missions. The cubesat standards have changed this to a certain extent. By following the standards and its requirements, the costs and development time of the preliminary design are cut. Then, it is possible to adopt different solutions to solve specific problems.

There are many companies selling 1U, 2U and 3U cubesat structures. Those are the most common, however, the cubesat market is expanding, naturally the need for different formats arises, so today, the cubesat development is heading for bigger cubesats. Many of the specialized cubesat companies have developed 6U structures. There are also 8U, 12U and 16U structures being both commercialized and developed, however, these formats are less common and are usually customized according to the client's needs.

### 1.2. Metal Sheet Folding

Pumpkin Inc. is a pioneer in the cubesat market. They have been commercializing cubesat products since 2000. Pumpkin's 1U, 2U and 3U structures have a main chassis, a base plate and a cover plate which adopt a riveted aluminium sheet folding approach. Using this solution, the loads are carried by the skin, the internal available volume is maximized and the strength to weight ratio is great. On the other hand, the required design tolerances may be difficult to respect because of the bending process. Regarding the riveting, although it ensures a great fastening capability, it may limit the assembly process.

### 1.3. Modular Frame Designs

ISIS SPACE developed a family of highly adaptable modular structures ranging from 1U to 16U configurations based on the Cubesat Standards. The structures are machined from an aluminium alloy, feature several mounting configurations to satisfy the needs of different customers, comply with the PC/104 form factor. While the frame carries most of the loads, the detachable panels carry the shear stress and allow access to the spacecraft avionics facilitating also the assembly and integration processes. The larger platforms may be customized according to the customer's requests.

### 1.4. Card Slot Design

Complex Systems and Small Satellites (C3S) is a Hungarian company created in 2012 to developed hardware and software solutions in the cubesat market. C3S developed a 3U and a 6U structures whose philosophy is a card slot system. This approach

makes it easier to access individual cards during the assembly, integration and testing procedures, than the classic PC/104 solution. According to C3S and the European Space Agency (ESA) the 3U structure will fly in late 2019 , being part of RadCube, a cubesat mission to demonstrate miniaturized technologies that measure in-situ the space radiation and magnetic field environment in low-earth orbit (LEO) for space weather monitoring purposes as part of ESA's Cubesat Technology Development activities.

### 1.5. Additive Manufacturing - 3D Printed Structures

Additive manufacturing technology frees the designer from the constraints of the traditional manufacturing methods, allowing for CAD models to be built by adding materials layer by layer. This process helps to speed up product development. Although it has been proposed for years for primary structures, only recently it has actually been implemented in a few projects.

Students at Tomsk Polytechnic University (TPU) developed a 3U cubesat, weighting 5kg to test new space materials technology. The entire casing of the satellite is 3D printed. The small satellite was launched to the International Space Station (ISS) in March 2016, where it performed a series of tests to assess its behaviour. On August 2017, the 3D printed spacecraft was deployed manually from the ISS. This was the first project to demonstrate that it is possible to use additive manufacturing on primary small satellite structures.

## 2. Numerical Analysis

To study the structure's behaviour when subjected to the launcher loads both static and dynamic analysis will be performed. This chapter comprehends the theoretical background behind said analyses.

### 2.1. Quasi-Static Numerical Analysis

Quasi-static analyses differ from dynamic analyses because the dynamic behaviour of the response is negligible due to the small variation that exists with time. The quasi-static loads are equivalent to static loads, typically expressed by equivalent accelerations in the centre of gravity (CoG).

This analysis aims to calculate the stresses, strains and displacements in the satellite when subjected to the accelerations presented in Table 4.

Considering linear materials and considering the theory of linear tension [5], the relation between the stress and the strain is given by:

$$\{\sigma\} = [D]\{\epsilon^{el}\} \tag{1}$$

where $\{\sigma\}$ is the stress vector, $[D]$ is the elasticity matrix defined by the material properties, $\{\epsilon^{el}\}$ is the elastic strain vector. Strains can be calculated by inverting equation (1):

$$\{\epsilon\} = [D]^{-1}\{\sigma\} \tag{2}$$

where $[D]^{-1}$ must be positive definite.

Displacements are calculated based on the infinitesimal strain tensor definition:

$$\boldsymbol{\epsilon} = \frac{1}{2}[\nabla \mathbf{u} + (\nabla \mathbf{u})^{\mathbf{T}}] \tag{3}$$

where $\boldsymbol{\epsilon}$ is the infinitesimal strain tensor, $\mathbf{u}$ represents the displacements and $\nabla$ is the differential operator.

### 2.2. Modal Numerical Analysis

The objective of the modal analysis carried out within this work is to determine the natural frequencies of the system. The natural frequency of a system is the frequency of a harmonic motion that characterizes its natural mode. In a modal analysis the system is considered linear, so, the stiffness and mass effects are constant, plus, the forces, displacements, pressures and temperatures applied are independent of time.

According to [6] the equation of motion with no damping and with no external applied forces is:

$$[M]\{\ddot{u}\} + [K]\{u\} = 0 \tag{4}$$

where $[M]$ is the mass matrix and $[K]$ is the system's stiffness matrix. $\{u\} = \{\Phi\}_i \cos(\omega_i t)$. $\{\Phi\}$ is the eigenvector that represents the mode shape of the $i_{th}$ natural frequency, $\omega_i$ is the natural angular frequency $[rad/s]$ and $t$ is time. Thus, equation (4) takes the form:

$$\Big(-\omega_i^2[M] + [K]\Big)\{\Phi\}_i = 0 \tag{5}$$

Equation (5) has two solutions that satisfy it. One is trivial and has no interest for the analysis, the other is obtained if the determinant of $\Big([K] - \omega^2[M]\Big)$ is equal to zero:

$$\big|[K] - \omega^2[M]\big| = 0 \tag{6}$$

Solving the previous eigenvalue problem we obtain the angular natural frequencies for each mode. The natural frequencies, $f_i$, are obtained from their direct relation with the natural angular frequencies:

$$f_i = \frac{\omega_i}{2\pi} \tag{7}$$

### 2.3. Harmonic Numerical Analysis

The harmonic numerical analysis evaluates the response of a system when excited by a harmonic vibration. In this type of analysis the system has constant stiffness, damping and mass effects. All

displacements vary harmonically at the same frequency, although they may have different phases.

To calculate the system's response when subjected to a harmonic load the mode superposition method was used. It takes advantage of the natural frequencies and mode shapes previously calculated in the modal analysis to decrease the computational time. In this method, the motion equation is converted into a modal form:

$$\ddot{y}_j + 2\omega_j \xi_j \dot{y}_j + \omega_j^2 y_j = f_j \tag{8}$$

where $y_j$ is the modal coordinate , $\omega_j$ is the natural angular frequency of mode $j$, $\xi_j$ is the fraction of critical damping for mode $j$ and $f_j$ is the force in modal coordinates.

For steady harmonic vibrations, $f_j$ has the form:

$$f_j = f_{jc} e^{i\Omega t} \tag{9}$$

where $f_{jc}$ is the complex force amplitude and $\Omega$ is the imposed angular frequency.

For equation (8) to be true at all times, $y_j$ must have a similar form as $f_j$:

$$y_j = y_{jc} e^{i\Omega t} \tag{10}$$

where $y_{jc}$ is the complex amplitude of the modal coordinate for mode $j$.

Differentiating equation (10), substituting equations (9) and (10) into equation (8), and solving for $y_{jc}$:

$$y_{jc} = \frac{f_{jc}}{\left(\omega_j^2 - \Omega^2\right) + i\left(2\omega_j \Omega \xi_j\right)} \tag{11}$$

The contribution for each mode is:

$$\left\{C_j\right\} = \left\{\phi_j\right\} y_{jc} \tag{12}$$

where $\left\{C_j\right\}$ is the contribution of mode $j$ and $\phi_j$ is the mode shape of mode $j$.

Finally, the displacement are obtained from $\left\{u\right\} = \sum_{i=1}^{n} \left\{\phi_i\right\} y_i$ as:

$$\left\{u_c\right\} = \sum_{j=1}^{n} \left\{C_j\right\} \tag{13}$$

where $\left\{u_c\right\}$ is the displacements vector.

2.4. Random Numerical Analysis

Random vibrations are non-deterministic. These are vibrations containing frequencies whose instantaneous magnitude cannot be explicitly defined. A random vibration analysis takes into account the excitation of all frequencies in a given spectrum, with the initial phase and magnitude of each frequency being random [6] .

This spectrum is presented as power spectral density (PSD) which is statistically originated from a large set of data collected from various measurements taken during the repetition of the event of interest. The shape of the graph represents the average acceleration of the signal at any frequency. The area under the curve is the mean acceleration of the signal squared and its square root is called the root-mean-squared (RMS) of the signal.

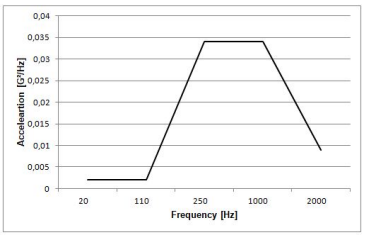


Figure 2: Input PSD profile $\left[Hz\right] vs \left[\frac{g^2}{Hz}\right]$

It is also necessary to define the probability density function (PDF). It allows to predict the range of accelerations that will be output. The area under the curve has probability 1. The area under PDF curve and between two $\left[G\right]$ values is the signal's probability of being in that range of accelerations.

The horizontal axis of PDF has $\left[Gpeak\right]$ units, which is normalized by dividing the $\left[G\right]$ values by the signal's RMS value. The signals usually have a bell shape form where 68.27% of the curve is between $\pm\sigma$ and 99.73% is between $\pm 3\sigma$.

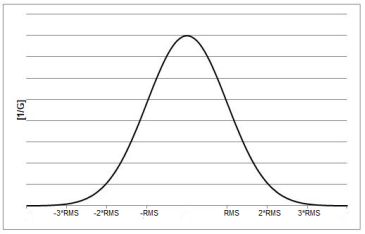


Figure 3: PDF Example

Most controllers consider that the control signal is a Gaussian distribution in which most of the intangible accelerations fall within the range of $\pm 3\sigma$. This removes the peak accelerations that represent the most danger to the system being analysed. Despite its limitations, the Gaussian model is the most widely used and will also be used in this work.

## 3. Design Concept Generation

A classical subsystem design approach was taken as presented in [8]. First, a list of requirements and constraints was done, then the preliminary design approach and overall configuration was chosen, the third step was to estimate the mass budget, afterwards a preliminary design was developed and finally, a baseline spacecraft configuration was created.

### 3.1. Requirements

The requirements derive from the mission and project constraints, as such, INFANTE's requirements are based on the cubesat ones [4], but are adapted and supplemented according to mission constraints. Following are the general structure requirements for INFANTE:

- R-D-001 The INFANTE satellite shall be designed according to 16U configuration.
- R-D-002 The total mass of the INFANTE satellite at launch, including the separation adaptor, shall be less than 25kg.
- R-D-003 No single point of failure shall lead to catastrophic or critical events.
- R-D-004 The structure, including all fasteners and launch separation mechanism shall be less than 3kg.
- R-D-005 The structure shall be a rectangular prism with the following dimensions 454 x 267 x 234 [mm].
- R-D-006 The system's first natural frequency shall be above 120Hz.
- R-D-007 The structure shall be compatible with the loads defined by the LVE.
- R-D-008 The structure shall be compatible with modules following the PC/104 standards.
- R-D-009 The spacecraft C.o.G shall be located within 4.5cm from its geometric centre (G.C) in the X and Y directions, and within 7 cm from its G.C in the Z direction.

In addition to these requirements there are several others for each subsystem that will not be presented because they are not relevant to this paper.

### 3.2. Design Approach, Materials and Fastening Methods

The main goals during development are to create a robust and lightweight structure that guarantees the physical integrity of all subsystems. One of the main drivers to INFANTE is modularity [7].

The spacecraft has 16 modules, each module has dimensions similar to a 1U cubesat, compatible with printed circuit boards (PCB) featuring the PC/104 connector. A drilling pattern was then created having in mind the maximization of volume between modules to facilitate harnessing.

Figure 4 and Figure 5 show the drilling pattern on the bottom plates and lateral plates, respectively.

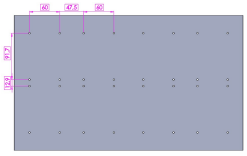

Figure 4: Drilling Pattern Bottom Plate [mm]

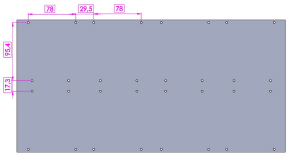

Figure 5: Drilling Pattern Lateral Plate [mm]

The chosen design approach was to have a primary structure composed by seven aluminium sheets; two for the $\pm X$ faces (Top and Bottom plates), two for the $\pm Y$ faces (lateral plates), two for the $\pm Z$ faces (prism bases) and another one to make an internal panel that concedes strength and robustness to the structure, while also facilitating the interface of some modules.

The aluminium sheets are machined, in Tekever's Ponte de Sor facility, so that the final panels are composed by the longitudinal stringers together with transverse skin (skin-stringer structures). The lateral panels carry bending moments, shear forces and torsional loads which induce axial stress in the stringers and skin together with shear stress in the skin. Several holes are cut off the structures to save weight. The holes are filleted in the corners to avoid fracture due to stress concentration. One of the main features of these panels is that the rails are integral part of the $\pm X$ panels. This way we reduce the amount of bolts in the structure, therefore, decreasing the design complexity, saving mass, facilitating the assembly process and simplifying the integration process given that we only have to unbolt one panel to have access to any module.

Figure 6 shows the seven panels (prior to machining):

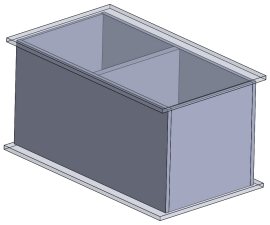

Figure 6: Panels Prior to Machining

Materials are selected based on several different characteristics, such as strength, stiffness, density, thermal, conductivity, thermal expansion, corrosion resistance, ductility, fracture toughness, ease of fabrication, versatility of attachment options, availability and cost [8]. For cubesats and small satellites, aluminium is a widely used material, however, materials such as steel or titanium are also used in some cases.

For INFANTE, it is important to have a material with a high strength-to-weight ratio, that is readily available and it's low cost. For those reasons, the material chosen for INFANTE's structure was an aluminium alloy. Even though steel is also a low cost material, its strength-to-weight is usually lower than aluminium because of it's higher density. For the same mass, aluminium shell or plate would be thicker and thus able to carry greater compressive loads before it buckles. Also, steel has magnetic properties which can easily interfere with instruments such as magnetorquers [2]. As for titanium , although it's strength-to weight ratio is similar to aluminium, it is much harder to machine.

7075-T6 is the aluminium alloy chosen for the INFANTE structure because it is flight proven and it has a high yield tensile strength which means that higher loads may be applied to the structure before the material enters in plastic state.

To attach structural elements, adhesive bonds, welds and mechanical fasteners are the most common methods. Mechanical fastener methods have a much higher impact on the mass budget than the other ones and allow for stress concentrations around the fasteners that can cause failure at lower load levels. However, by well dimensioning the structure and respecting the norms regarding these kind of fasteners, it is possible to get around this issue. The fact that it is possible to disassemble two bolted parts, makes it the best fit for INFANTE.

The primary and secondary structures will be bolted together using space graded bolts. These bolts are not procured or chosen yet, nor are the nuts, but Tekever has been in contact with fastener provider Johann Maier GmbH &Co.KG to find the best fit for INFANTE's needs. Tables 1 and 2 present, respectively, a selection of potential bolts and nuts to be used (available in stainless steel and titanium):

| Bolt | Size |
|---|---|
| ISO 4762 | M2/M3/M4 |
| ISO 14583 | M2.5/M3/M4 |

Table 1: Potential bolts to be used in INFANTE

| Nuts | Size |
|---|---|
| ISO 7092 | M2.5/M3/M4 |
| DIN 934 | M4 |

Table 2: Potential nuts to be used in INFANTE

### 3.3. Configuration

The internal arrangement has to use the available space in the most efficient way possible, it has to take in consideration the performance constraints of each subsystem and also take in consideration the electric, magnetic, mechanical and thermal interfaces. It needs to take in consideration the assembly and integration processes. Thus, finding the ideal internal arrangement in a spacecraft is a very demanding task. As it is heavily dependent on every subsystem, it is not possible to define the internal arrangement at this point in the development process. However, it is possible to establish a baseline arrangement based on solid assumptions.

To respect R-D-009 the weight has to be evenly distributed. The tactic used is to put heavy components near the G.C. This tactic also has a positive impact in inertia, decreasing it, which helps the ADCS to control the spacecraft's attitude.

Figure 7 shows the INFANTE's structure preliminary design.

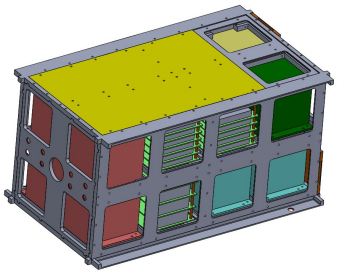

Figure 7: INFANTE's structure preliminary design

### 3.4. Total Mass

Table 3 presents the mass of each subsystem featured in the computational model.

| Subsystem | Total Mass [g] |
|---|---|
| Primary Structure | 3698 |
| Secondary Structure | 1344 |
| Propulsion | 3000 |
| Battery Packs | 1936 |
| OBC | 200 |
| OBDH | 200 |
| Gammalink | 600 |
| SAR radio | 200 |
| PCDU | 700 |
| PDRU | 1200 |
| ADCS Core Unit | 1000 |
| Reaction Wheels | 360 |
| Multispectral Camera | 2000 |
| Solar Panels | 394 |
| Communications Antennas | 170 |
| Payload Computer | 85 |
| Experiments Unit | 1000 |
| System Total Mass [g] | 18,087.0 |

Table 3: System Mass

The system's total mass is 18.087kg and it will definitely increase. There are subsystems that at this point surpass the maximum required mass.

However it is expected that their mass will decrease with future iterations of their development.

## 4. Computational Modelling Analysis and Results Discussion

All simulations were performed using ANSYS 18.1 Workbench software.

### 4.1. Computational Model

To decrease the computational time two major simplifications were made: all the fillets and chamfers were suppressed; the subsystems were modelled as mass points. These have the same mass and are located at the centres of mass of the respective subsystems and are attached to the rods by one dimension (1D) elements. Mass points do not take the geometry in consideration and do not allow to define the connections as the preliminary subsystems' CAD models would, which influence the results. Because of its limitations mass points should not be considered as representations of the subsystems after the PDR phase. Nevertheless, these assumptions have the advantages of decreasing the number of mesh elements in the order of millions and allow to study the structure's behaviour before the preliminary designs of every subsystem are ready.

### 4.2. Boundary Conditions

The computational model used has the same boundary conditions for all simulations. The boundary conditions depend on the design of the satellite interface with the launcher. In INFANTE's case, the existing interface that hosts the satellite during the launch is a picosatellite orbital deployer (POD).

The POD will have an approximately prismatic shape. It will have a cage-like structure, which is not completely closed. The POD is connected to the satellite and to an adapter which is connected to the launcher.

The boundary conditions are: 6 fixed point total, four in the -Z face (in red) and two in the -X face. There are four edges (in blue) that are free in the Z direction but cannot move in neither X and Y direction nor rotate. Figure 8 represents the boundary conditions in the computational model.

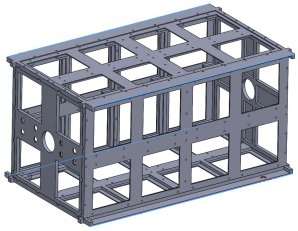

Figure 8: Computational model boundary conditions

### 4.3. Applied Loads

The load profiles to performed the analysis are provided by the launcher entity and are presented in Tables 4, 5 and 6.

| Quasi-static loads | Loads $[g]$ |
|---|---|
| Main Structure | 10.05 |

Table 4: Quasi-static qualification load profile

| | Freq. $[Hz]$ | Qual. |
|---|---|---|
| Structure | 5-8 | 1.15g |
| | 8-100 | 3g |
| Sweep Rate | | 2 Oct/min |

Table 5: Harmonic qualification load profile

| | Freq. [Hz] | PSD $[g^2/Hz]$ |
|---|---|---|
| Each axis | 20 | 0.002 |
| | 110 | 0.002 |
| | 250 | 0.034 |
| | 1000 | 0.034 |
| | 2000 | 0.009 |
| g RMS | | 6.7 |
| Duration | | 2 min/axis |

Table 6: Random vibration qualification load profile

### 4.4. Mesh Generation

ANSYS offers a wide variety of elements that fit different needs. Considering the computational model and the simulations planed, the elements chosen are shown in Table 7. The mechanical properties of aluminium 7075-T6 were assigned to all mesh elements.

The computational model mesh was constituted by elements 1D, 2D and 3D:

- 1D elements were used to represent the rods of the PCB stacks, screws and the connections between different parts.
- 2D elements were used to represent parts idealized as surfaces.
- 3D elements were used to represent parts idealized as solids.

| Part | Element Type |
|---|---|
| Stack's rods | Beam188 |
| Screws | Beam188 |
| Structural Panels | Shell181 |
| Sec. Structure (Solid) | Solid185 |
| Sec. Structure (Surface) | Shell181 |

Table 7: Mesh element types per part

### 4.5. Static Analysis Results

During the static analysis the spacecraft was positioned horizontally, a $10.05g$ acceleration was applied on the spacecraft's C.o.G in each axis at a time. Figures 9, 10 and 11 show the maximum displacement, maximum Von-Mises stress and maximum Von-Mises strain. Note that the figures presented only concern the analysis performed with the loads applied in the $zz$ direction. The maximum values were registered when the loads were applied in said direction, therefore, these simulations are considered critical. Table 8 shows the maximum deformation, stress and strain values for the simulations in each direction.

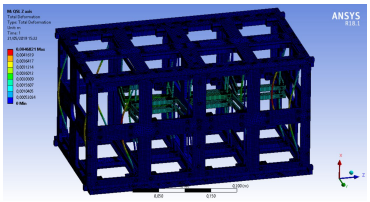

Figure 9: Structure's deformation during QSL on $zz$ direction

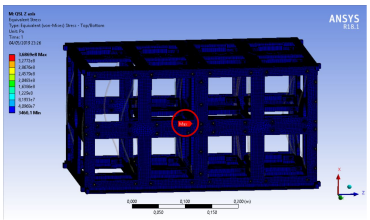

Figure 10: Structure's Von-Mises stress during QSL on $zz$ direction

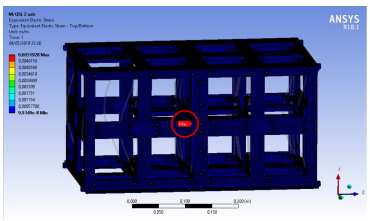

Figure 11: Structure's Von-Mises strain during QSL on $zz$ direction

| Axis | $xx$ | $yy$ | $zz$ |
|---|---|---|---|
| Max Def. $[mm]$ | 0.420 | 4.58 | 4.68 |
| Max Stress $[MPa]$ | 272.82 | 248.14 | 368.69 |
| Max Strain | 0.0041 | 0.0035 | 0.0052 |

Table 8: QSL maximum diplacements, stresses and strains

During launch the body structure has a maximum displacement of 4.68 $mm$ when the load is applied in the $zz$ direction.

Figures 10 and 11 show that the stress and strain are quite uniform throughout the structure and that the maximum values occur in the stack frames where the rods are fixed. The maximum stress and strain values are 368.69 $MPa$ and 0.0052, receptively. The tensile yield strength and the elongation at break of aluminium 7075-T6 are 503 $MPa$ and 11% which are above the maximum values registered by the analysis, giving a safety factor of $S_f = \frac{503}{368.57} = 1.36$.

### 4.6. Modal Analysis Results

No loads were applied during the execution of this analysis. Figure 12 shows the displacement on the first vibration mode:

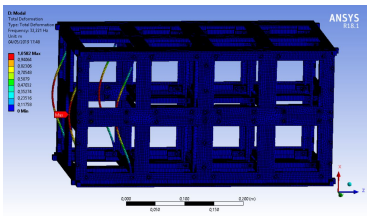

Figure 12: Structure's deformation during modal analysis

The first vibration mode occurs at a natural frequency of 32.221 $Hz$, making the propulsion stack enter in resonance. Given that the first natural frequency shall be above $120Hz$, it is clear that actions need to be taken so that the first natural mode is in compliance with the requirements. The two main reasons that contribute for such low values are:

- **Early stage of development** At this stage, there are several open points regarding the design of the structure, thus, it is natural that results may not be ideal.
- **Over simplifications of the model** Ideally the computational model would be the same as the design model and would include all the systems details. However, due to the dimensions of the spacecraft, the still roughly developed design of the subsystems, a limited time frame and limited computational capacity available, simplifications to the computational model needed to be made so that the development could progress. These simplifications, as mentioned in section 4.4, have a great impact on the results, specially the substitution of the subsystems design by mass points which contributes to a decrease in the system's stiffness.

However, these results offer good indication on how to move forward. The natural frequencies must

increase, otherwise requirement R-D-006 will not be respected. Equation (4) tells us that to influence the natural frequencies of a system there are two driving factors. The system's mas and stiffness. From the theory of dynamics we get equation (14), that tell us that natural frequencies of a system increase if the mass decreases for the same stiffness or if the stiffness increases for the same mass. Ideally we could increase the stiffness and decrease the mass. Fortunately, at this point both are possible. To increase the system's stiffness we can change the materials or the boundary conditions. It is unlikely that the structure's material will change in the future, because aluminium 7075-T6 is the best fit for INFANTE. As the spacecraft is in a early is stage of development there is flexibility to make significant changes to the structure's overall design, to the interface design and to the subsystems designs. The mass will decrease at each design iteration and structure optimization.

$$f_{nat} = \frac{1}{2\pi}\sqrt{\frac{k}{m}} \tag{14}$$

### 4.7. Harmonic Analysis Results

The harmonic vibrations analyses were performed to determine the stress and displacements of the structure when subjected to the harmonic excitations described in Table 5. The analysis were performed considering the excitations applied in each one of the three orthogonal directions independently.

Figures 13 and 14 show the deformation and the equivalent stress in the structure when the excitations are applied on the $yy$ (critical analysis).Table 9 shows the maximum displacements and stress values.

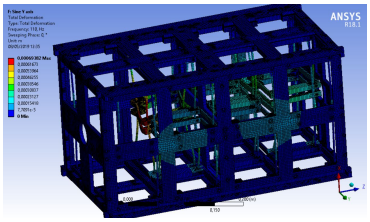

Figure 13: Structure's deformation during harmonic analysis on $yy$ direction

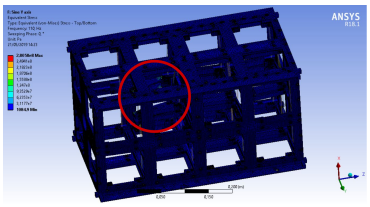

Figure 14: Structure's stress during harmonic analysis on $yy$ direction

| Axis | $xx$ | $yy$ | $zz$ |
|---|---|---|---|
| Max Def. $[mm]$ | 0.168 | 0.694 | 0.362 |
| Max Stress $[MPa]$ | 92.8 | 280.5 | 81.5 |

Table 9: Harmonic maximum displacements and stresses

The displacements and the stresses in each simulation are relatively small. The maximum values recorded occur in the secondary structure. As showed in Table 9 the maximum stress is $280.5\left[MPa\right]$ which means that the structure is at all times in the linear state, therefore, it never enters in a plastic or rupture state. The lowest safety factor for these analysis is in the $yy$ direction, $Sf = \frac{503}{280.5} = 1.79$.

### 4.8. Random Vibration Analysis Results

The random vibrations analyses were performed to determine the acceleration and the stress on the structure when subjected to random excitations as described in Table 6 and represented in Figure 2.

Figure 15 shows the body directional acceleration results when the random excitations are applied in the $yy$ direction.

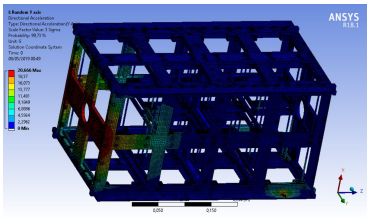

Figure 15: Directional Acceleration. Random vibrations in $yy$ direction

Figure 16 show the body equivalent stress when the random vibrations are applied in the $zz$ direction.

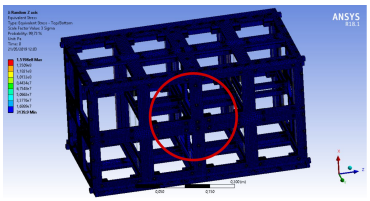

Figure 16: Stress under random vibrations in $zz$ direction

Table 10 show the maximum acceleration and stress values for each analysis.

| Axis | $xx$ | $yy$ | $zz$ |
|---|---|---|---|
| Acceleration $[G]$ | 20.303 | 20.666 | 2.928 |
| Max Stress $[MPa]$ | 14.3 | 7.85 | 151.98 |

Table 10: Random vibrations maximum accelerations and stresses

There's only a 0.27% probability of accelerations to exceed $20.666\big[G\big]$, when excitations are applied in the $yy$ direction. This probability is a consequence of using the Gaussian model and $3\sigma$. There is a 99.73% probability of the maximum equivalent stress not exceed $151.98\big[MPa\big]$ when the loads are applied in the $zz$ direction. These values are all below the material's yield stress. The safety factor is $Sf = \frac{503}{151.98} = 3.3$, therefore we can conclude that no structural harm will be done to the structure because of random vibrations.

## 5. Conclusions and Future Work

This work provides Tekever with a preliminary design of a smallsat structure while capturing its development process. It is relevant for the company to bridge the knowledge gap to more established competitors. The work developed adds experience and expertise on small spacecraft design and provides a firm baseline that allows the company to speed up the structure design process for future smallsats. This work accomplished all the initially proposed goals as INFANTE has now a preliminary design for its structural subsystem which is ready to be iterated and improved as the project progresses.

### 5.1. Future Work

This work is the first step of INFANTE's structural subsystem development. As the project progresses the design will be iteratively refined. The next suggested next steps are as follows:

- It is necessary to increase the structure's natural frequencies. The first step is to increase the representativeness of the computational model by including the other subsystems' computational models on the existent one. Then a modal analysis should be run to check if the natural frequencies increased to satisfying levels. Depending if they did or not different approaches are taken.
- Assuming that the natural frequencies are not yet high enough a design solution should be implemented. Said design solution can be focused on two variables, stiffness or mass. The interface between the structure and the subsystems could be redesigned to increase the structure's overall stiffness.
- We can then run a topology analysis where the aim is to decrease the mass of the subsystem without compromising structural performance.
- If as consequence of increasing the model representativeness the natural frequencies are satisfying, we can remove material to decrease the structure's mass thus optimizing the internal volume available, production and launching costs.
- Afterwards the static, harmonic and random vibrations analyses should be performed again to make sure that the structure survives under such loads.

After these steps, the structure model will need to be produced and go through experimental testing to validate the simulations results.


## Acknowledgements

I would like to thank Professor Filipa Moleiro, Eng. Francisco Vilhena da Cunha, Eng. Vitor Cristina, Rui Santos, Eng. Marie Campana and Eng. Carlos Dias.


## References


[1] Nanosats Database. https://www.nanosats.eu/ (Accessed on 2 March 2019).

[2] Technical report, European Cooperation for Space Standardization. ECSS-E-HB-20-07A – Electromagnetic Compatibility Handbook, 2012.

[3] California Polytechnic State University. Poly Picosatellite Orbital Deployer user Guide Mk. III Rev E, March 2014.

[4] California Polytechnic State University. CubeSat Design Specification Revision 13, April 2015.

[5] A. M. Barros. Behaviour Law PDF, Instituto Superior Técnico, 2016.

[6] S. Rao. *Mechanical Vibrations*. Prentice Hall, $5^{th}$ edition, 2011.

[7] Tekever. Infante system design and justification. October 2018.

[8] J. Wertz. *Space Mission Analysis and Design*. Kluwer Academic Publishers, $3^{th}$ edition, 1999.